EUROPEAN ORGANISATION FOR NUCLEAR RESEARCH

CERN-PPE/95-83
7th June, 1995

Investigation of the String Effect using Final State Photons

The OPAL Collaboration

Abstract

The string effect in QCD is investigated using data from the OPAL detector at LEP. By comparing the charged particle flow in three-jet multihadronic events with that in events with two jets and a hard isolated photon, the sensitivity to particular models is reduced. A comparison with various Monte Carlo models is presented. The difference in particle flows in the interquark region is found to be well reproduced by a leading order calculation of soft gluon emission, in the spirit of the Local Parton Hadron Duality hypothesis.

(Submitted to Z.Phys.C)

The OPAL Collaboration

R. Akers[16], G. Alexander[23], J. Allison[16], N. Altekamp[5], K. Ametewee[25], K.J. Anderson[9], S. Anderson[12], S. Arcelli[2], S. Asai[24], D. Axen[29], G. Azuelos[18,a], A.H. Ball[17], E. Barberio[26], R.J. Barlow[16], R. Bartoldus[3], J.R. Batley[5], G. Beaudoin[18], J. Bechtluft[14], A. Beck[23], G.A. Beck[13], C. Beeston[16], T. Behnke[27], K.W. Bell[20], G. Bella[23], S. Bentvelsen[8], P. Berlich[10], S. Bethke[14], O. Biebel[14], I.J. Bloodworth[1], P. Bock[11], H.M. Bosch[11], M. Boutemeur[18], S. Braibant[12], P. Bright-Thomas[25], R.M. Brown[20], A. Buijs[8], H.J. Burckhart[8], C. Burgard[27], R. Bürgin[10], P. Capiluppi[2], R.K. Carnegie[6], A.A. Carter[13], J.R. Carter[5], C.Y. Chang[17], C. Charlesworth[6], D.G. Charlton[1,b], S.L. Chu[4], P.E.L. Clarke[15], J.C. Clayton[1], S.G. Clowes[16], I. Cohen[23], J.E. Conboy[15], O.C. Cooke[16], M. Cuffiani[2], S. Dado[22], C. Dallapiccola[17], G.M. Dallavalle[2], C. Darling[31], S. De Jong[12], L.A. del Pozo[8], H. Deng[17], M.S. Dixit[7], E. do Couto e Silva[12], J.E. Duboscq[8], E. Duchovni[26], G. Duckeck[8], I.P. Duerdoth[16], U.C. Dunwoody[8], J.E.G. Edwards[16], P.G. Estabrooks[6], H.G. Evans[9], F. Fabbri[2], B. Fabbro[21], M. Fanti[2], P. Fath[11], F. Fiedler[12], M. Fierro[2], M. Fincke-Keeler[28], H.M. Fischer[3], R. Folman[26], D.G. Fong[17], M. Foucher[17], H. Fukui[24], A. Fürtjes[8], P. Gagnon[6], A. Gaidot[21], J.W. Gary[4], J. Gascon[18], S.M. Gascon-Shotkin[17], N.I. Geddes[20], C. Geich-Gimbel[3], S.W. Gensler[9], F.X. Gentit[21], T. Geralis[20], G. Giacomelli[2], P. Giacomelli[4], R. Giacomelli[2], V. Gibson[5], W.R. Gibson[13], J.D. Gillies[20], D.M. Gingrich[30,a], J. Goldberg[22], M.J. Goodrick[5], W. Gorn[4], C. Grandi[2], E. Gross[26], G.G. Hanson[12], M. Hansroul[8], M. Hapke[13], C.K. Hargrove[7], P.A. Hart[9], C. Hartmann[3], M. Hauschild[8], C.M. Hawkes[8], R. Hawkings[8], R.J. Hemingway[6], G. Herten[10], R.D. Heuer[8], J.C. Hill[5], S.J. Hillier[8], T. Hilse[10], P.R. Hobson[25], D. Hochman[26], R.J. Homer[1], A.K. Honma[28,a], R. Howard[29], R.E. Hughes-Jones[16], D.E. Hutchcroft[5], P. Igo-Kemenes[11], D.C. Imrie[25], A. Jawahery[17], P.W. Jeffreys[20], H. Jeremie[18], M. Jimack[1], A. Joly[18], M. Jones[6], R.W.L. Jones[8], P. Jovanovic[1], J. Kanzaki[24], D. Karlen[6], K. Kawagoe[24], T. Kawamoto[24], R.K. Keeler[28], R.G. Kellogg[17], B.W. Kennedy[20], B.J. King[8], J. King[13], J. Kirk[29], S. Kluth[5], T. Kobayashi[24], M. Kobel[10], D.S. Koetke[6], T.P. Kokott[3], S. Komamiya[24], R. Kowalewski[8], T. Kress[11], P. Krieger[6], J. von Krogh[11], P. Kyberd[13], G.D. Lafferty[16], H. Lafoux[8], R. Lahmann[17], W.P. Lai[19], D. Lanske[14], J. Lauber[8], J.G. Layter[4], A.M. Lee[31], E. Lefebvre[18], D. Lellouch[26], J. Letts[2], L. Levinson[26], S.L. Lloyd[13], F.K. Loebinger[16], G.D. Long[17], B. Lorazo[18], M.J. Losty[7], J. Ludwig[10], A. Luig[10], A. Malik[21], M. Mannelli[8], S. Marcellini[2], C. Markus[3], A.J. Martin[13], J.P. Martin[18], T. Mashimo[24], W. Matthews[25], P. Mättig[3], J. McKenna[29], E.A. Mckigney[15], T.J. McMahon[1], A.I. McNab[13], F. Meijers[8], S. Menke[3], F.S. Merritt[9], H. Mes[7], A. Michelini[8], G. Mikenberg[26], D.J. Miller[15], R. Mir[26], W. Mohr[10], A. Montanari[2], T. Mori[24], M. Morii[24], U. Müller[3], B. Nellen[3], B. Nijjhar[16], S.W. O'Neale[1], F.G. Oakham[7], F. Odorici[2], H.O. Ogren[12], N.J. Oldershaw[16], C.J. Oram[28,a], M.J. Oreglia[9], S. Orito[24], F. Palmonari[2], J.P. Pansart[21], G.N. Patrick[20], M.J. Pearce[1], P.D. Phillips[16], J.E. Pilcher[9], J. Pinfold[30], D.E. Plane[8], P. Poffenberger[28], B. Poli[2], A. Posthaus[3], T.W. Pritchard[13], H. Przysiezniak[30], M.W. Redmond[8], D.L. Rees[1], D. Rigby[1], M.G. Rison[5], S.A. Robins[13], N. Rodning[30], J.M. Roney[28], E. Ros[8], A.M. Rossi[2], M. Rosvick[28], P. Routenburg[30], Y. Rozen[8], K. Runge[10], O. Runolfsson[8], D.R. Rust[12],

M. Sasaki[24], C. Sbarra[2], A.D. Schaile[8], O. Schaile[10], F. Scharf[3], P. Scharff-Hansen[8], P. Schenk[4], B. Schmitt[3], M. Schröder[8], H.C. Schultz-Coulon[10], M. Schulz[8], P. Schütz[3], J. Schwiening[3], W.G. Scott[20], M. Settles[12], T.G. Shears[16], B.C. Shen[4], C.H. Shepherd-Themistocleous[7], P. Sherwood[15], G.P. Siroli[2], A. Skillman[15], A. Skuja[17], A.M. Smith[8], T.J. Smith[28], G.A. Snow[17], R. Sobie[28], S. Söldner-Rembold[10], R.W. Springer[30], M. Sproston[20], A. Stahl[3], M. Starks[12], C. Stegmann[10], K. Stephens[16], J. Steuerer[28], B. Stockhausen[3], D. Strom[19], P. Szymanski[20], R. Tafirout[18], P. Taras[18], S. Tarem[26], M. Tecchio[9], P. Teixeira-Dias[11], N. Tesch[3], M.A. Thomson[8], E. von Törne[3], S. Towers[6], M. Tscheulin[10], T. Tsukamoto[24], A.S. Turcot[9], M.F. Turner-Watson[8], P. Utzat[11], R. Van Kooten[12], G. Vasseur[21], P. Vikas[18], M. Vincter[28], F. Wäckerle[10], A. Wagner[27], D.L. Wagner[9], C.P. Ward[5], D.R. Ward[5], J.J. Ward[15], P.M. Watkins[1], A.T. Watson[1], N.K. Watson[7], P. Weber[6], P.S. Wells[8], N. Wermes[3], B. Wilkens[10], G.W. Wilson[27], J.A. Wilson[1], T. Wlodek[26], G. Wolf[26], S. Wotton[11], T.R. Wyatt[16], G. Yekutieli[26], V. Zacek[18], W. Zeuner[8], G.T. Zorn[17].

[1]School of Physics and Space Research, University of Birmingham, Birmingham B15 2TT, UK
[2]Dipartimento di Fisica dell' Università di Bologna and INFN, I-40126 Bologna, Italy
[3]Physikalisches Institut, Universität Bonn, D-53115 Bonn, Germany
[4]Department of Physics, University of California, Riverside CA 92521, USA
[5]Cavendish Laboratory, Cambridge CB3 0HE, UK
[6]Carleton University, Department of Physics, Colonel By Drive, Ottawa, Ontario K1S 5B6, Canada
[7]Centre for Research in Particle Physics, Carleton University, Ottawa, Ontario K1S 5B6, Canada
[8]CERN, European Organisation for Particle Physics, CH-1211 Geneva 23, Switzerland
[9]Enrico Fermi Institute and Department of Physics, University of Chicago, Chicago IL 60637, USA
[10]Fakultät für Physik, Albert Ludwigs Universität, D-79104 Freiburg, Germany
[11]Physikalisches Institut, Universität Heidelberg, D-69120 Heidelberg, Germany
[12]Indiana University, Department of Physics, Swain Hall West 117, Bloomington IN 47405, USA
[13]Queen Mary and Westfield College, University of London, London E1 4NS, UK
[14]Technische Hochschule Aachen, III Physikalisches Institut, Sommerfeldstrasse 26-28, D-52056 Aachen, Germany
[15]University College London, London WC1E 6BT, UK
[16]Department of Physics, Schuster Laboratory, The University, Manchester M13 9PL, UK
[17]Department of Physics, University of Maryland, College Park, MD 20742, USA
[18]Laboratoire de Physique Nucléaire, Université de Montréal, Montréal, Quebec H3C 3J7, Canada
[19]University of Oregon, Department of Physics, Eugene OR 97403, USA

[20]Rutherford Appleton Laboratory, Chilton, Didcot, Oxfordshire OX11 0QX, UK
[21]CEA, DAPNIA/SPP, CE-Saclay, F-91191 Gif-sur-Yvette, France
[22]Department of Physics, Technion-Israel Institute of Technology, Haifa 32000, Israel
[23]Department of Physics and Astronomy, Tel Aviv University, Tel Aviv 69978, Israel
[24]International Centre for Elementary Particle Physics and Department of Physics, University of Tokyo, Tokyo 113, and Kobe University, Kobe 657, Japan
[25]Brunel University, Uxbridge, Middlesex UB8 3PH, UK
[26]Particle Physics Department, Weizmann Institute of Science, Rehovot 76100, Israel
[27]Universität Hamburg/DESY, II Institut für Experimental Physik, Notkestrasse 85, D-22607 Hamburg, Germany
[28]University of Victoria, Department of Physics, P O Box 3055, Victoria BC V8W 3P6, Canada
[29]University of British Columbia, Department of Physics, Vancouver BC V6T 1Z1, Canada
[30]University of Alberta, Department of Physics, Edmonton AB T6G 2J1, Canada
[31]Duke University, Dept of Physics, Durham, NC 27708-0305, USA

[a]Also at TRIUMF, Vancouver, Canada V6T 2A3
[b] Royal Society University Research Fellow

1 Introduction

Previous studies [1, 2] of three-jet events in e^+e^- annihilation experiments have provided evidence for a depletion of the particle flow in the region between the quark and anti-quark jets relative to that between the quark and gluon jets. This has come to be known as the "string effect".

This effect is predicted by the Lund string model [3], one of the most successful models of hadronization. The Lund model pictures a string stretched between pairs of partons of opposite colour charge, and carrying the colour flux. In a $q\bar{q}g$ event, the doubly-coloured gluon is a kink on the string connecting the q and $\bar{q}$. Since the two string segments are boosted away from the interquark region, hadrons are preferentially produced between the $q(\bar{q})$ and the gluon, resulting in the string effect.

In perturbative QCD, the depletion of particle flow in the interquark region has been attributed to coherence effects due to soft gluon radiation from the colour dipoles formed by the primary partons [4]. The hypothesis of Local Parton Hadron Duality (LPHD) [5], which assumes that the angular distribution of final state hadrons reflects the flow of soft gluons, then implies that this quantum phenomenon of interference is sufficient to explain the string effect. Some Monte Carlo models also take this destructive interference into account, for example, by imposing angular ordering (i.e. the branching angles decrease as the shower evolves) or from azimuthal anisotropies in gluon radiation. These models have been called coherent parton shower models.

The string picture for fragmentation and QCD coherence effects could be partially complementary. Since one is forced to resort to parametrization in order to describe the process of combination of coloured partons to form colourless hadrons, the relative importance of the two phenomena is difficult to evaluate. It has been predicted that the string effect quickly becomes dominated by the perturbative phase of the jet evolution as the centre of mass energy increases [6].

The original method of demonstrating the string effect [1] is to compare the particle flow in the event plane of three-jet events, after energy ordering of the jets, with simulations based on two types of Monte Carlo generators: those that incorporate string fragmentation, and those that are based on independent fragmentation [7]. These studies have been criticized [8] for having made use, in the case of independent jet fragmentation, of the original simple Field-Feynman algorithm [9], with the conclusion that one could not exclude a kinematical origin for the observed effect.

Here, we exploit the power of photons as probes of QCD [10], and report on a method, first suggested by Azimov *et al.* [11], based on the comparison of charged particle flows in three-jet events ($q\bar{q}g$) to that in radiative two-jet events ($q\bar{q}\gamma$), produced in e^+e^- annihilation at $\sqrt{s} = M_{Z^0}$. In the $q\bar{q}\gamma$ sample, destructive interference should be absent, and the string configuration is different from that in the $q\bar{q}g$ sample. The LPHD hypothesis would then imply that, at the hadron level as well, one should find additional evidence for the string effect, i.e. a reduced charged particle density in the region between the two quark jets in $q\bar{q}g$ events, relative to the density between the two jets of $q\bar{q}\gamma$ events. The advantage of this method is that the interquark regions are compared directly, the only difference being that the other hemisphere of the event contains either a gluon or a photon. Unlike other methods [1], this one is not sensitive to possible differences between narrow quark and broad gluon jets. Therefore, the dependence of the observed string effect on Monte Carlo simulations is considerably reduced. In ref. [8], it has been pointed out that the difference in invariant mass between the radiated photon and the gluon jet in the two samples could account for the observed depletion in three-jet events. An attempt to answer this criticism is made here.

Model-independent evidence for the string effect, using quark tagging in 3-jet events with symmetrical quark-gluon jet configurations, has been reported by OPAL [2]. It established the string effect in an original fashion, addressing criticism of the earlier work in that quark and gluon jets were in symmetric configurations, and did not have the problem of different jet masses between gluon and photon. The present analysis, with $q\bar{q}\gamma$ data, complements that study by using a different approach and can be compared to analytical calculations based on simple models of soft gluon emission.

Similar analyses have been reported at lower energies [12–14] and in Z^0 decays at LEP [15]. In the present analysis, systematic effects are investigated, and predictions that the dependence on out-of-plane momentum is reduced at LEP energies [6] are tested.

2 The OPAL Detector and Event Selection

The OPAL detector and trigger system are described in ref. [16]. For the purposes of this study, the principal components are the central detector and the electromagnetic calorimeter. The first consists of a silicon microvertex detector [17], a vertex detector which is a precise drift chamber covering the range $|\cos\theta| < 0.95$ (where θ is the angle relative to the beam direction), a large volume jet chamber which provides tracking and ionization energy loss ($\mathrm{d}E/\mathrm{d}x$) information, and z-chambers which measure the coordinates, parallel to the beam, of charged tracks leaving the jet chamber within the range $|\cos\theta| < 0.72$. The barrel electromagnetic calorimeter is made up of lead-glass blocks, arranged on the surface of a cylinder of radius 2.45 m, and covers the angular range $|\cos\theta| < 0.82$. Each block of lead-glass is 24.6 radiation lengths deep and points towards the interaction point, subtending a solid angle of about 40 x 40 mrad^2. The endcap calorimeters cover the range $0.81 < |\cos\theta| < 0.98$.

For this analysis, approximately 2×10^6 multihadronic events from the OPAL data recorded between 1990 and 1993 were first selected as in ref. [18]. In addition, charged tracks were required to have more than 40 out of a maximum of 159 reconstructed hits in the jet chamber, a momentum transverse to the beam direction $p_T > 250$ MeV/c, and a minimum distance of less than 5 cm in the transverse plane and 30 cm in the longitudinal direction from the nominal interaction point. For about 4% of the events, charged tracks had a reconstructed momentum which was unphysically high: in this case, the whole event was rejected. Electromagnetic clusters were used if they had at least 250 MeV deposited in at least one block in the barrel region, or with more than one block in the endcap region. Only events with at least five charged tracks and seven electromagnetic clusters were kept for this study.

Events containing a final state photon were selected from the multihadron sample as follows (for details see ref. [19]). The photon candidates were required to be in the region $|\cos\theta| < 0.72$ and to have an energy greater than 7.5 GeV. They had to be isolated in the sense that no track or additional electromagnetic cluster was present inside a cone of half angle 15° around them. Clusters were required to be contained in fewer than 16 blocks and to have an energy-weighted width of less than 30 mrad. The shape variable for the cluster, defined in ref. [19], was used as a criterion to reject background from neutral hadrons, especially π^0 mesons. The residual background from neutral hadrons was estimated to be 7% [19].

For events which passed the multihadron selection criteria, jets were formed from the charged tracks and electromagnetic clusters using the Durham [20] algorithm based on the relative transverse momentum squared of particle clusters. A reference value for the jet parameter, y_{cut}= 0.007, was chosen. For the $q\bar{q}\gamma$ sample of final state photon events, the photon was removed from the event before the remaining tracks and clusters were subjected to the jet clustering algorithm, but the calculated visible energy included the photon energy. The photon was then reintroduced and treated as a third jet. The event was rejected if the effective value of y_{cut} between the photon and either of the other two jets fell below 0.007, i.e. the event was required to be reconstructed as a three-jet event with the photon considered to be a separate jet. Only three-jet events ($q\bar{q}g$) or radiative two-jet events ($q\bar{q}\gamma$) were accepted. Reconstructed jet energies were corrected according to a parametrization procedure for double counting of momentum and energy obtained from the jet chamber and electromagnetic calorimeters. Evaluation of their energies from the interjet angles assuming massless kinematics was also used, but no significant difference was observed on the measurement of the string effect. Because of the difference in the masses of the photon and gluon jets, direct experimental measurement of the jet energies is likely to be a less biased method.

Selection criteria were applied to the jets. They were required to consist of at least four particles (charged tracks and electromagnetic clusters). As it will be assumed in section 3 that the lowest energy jet in the $q\bar{q}g$ sample is the gluon jet, events were rejected if the least energetic jet fell outside the region $|\cos\theta| > 0.72$, so that the gluon jet selection was analogous to the photon selection. (It was verified that this last cut had a negligible effect on the measurement of the string effect.) Finally, only events in which the third jet had an energy below 28 GeV were used, since there were no photons above that energy in the $q\bar{q}\gamma$ sample: only $q\bar{q}\gamma$ events where the photon was less energetic than both of the jets were kept. A coplanarity condition based on the angles between jets was imposed: $\sum_{i \neq j} \theta_{ij} > 358°$. In order to minimize the effect of jets with poorly reconstructed energy, events where the two highest energy jets had an opening angle below 120° were rejected. After all these cuts, the radiative two-jet sample ($\mathrm{q\bar{q}}\gamma$) consisted of 1280 events and the three-jet hadronic sample ($\mathrm{q\bar{q}g}$) of 285,400 events.

3 Measurement of the String Effect

The jets of the $\mathrm{q\bar{q}g}$ and $\mathrm{q\bar{q}}\gamma$ samples were ordered in decreasing energy. An event plane was defined as the one spanned by the two eigenvectors of the sphericity tensor [21] which correspond to the two largest eigenvalues. The charged particle flow in this event plane was then constructed as a function of the azimuthal angle, starting from the highest energy jet (jet 1) and continuing in the direction of the jet with the second highest energy (jet 2). The third, least energetic jet, has a high probability of being derived from the gluon (see below).

Fig. 1a shows the resulting charged particle flow. The histogram is normalized to represent the number of charged particle tracks per accepted event per angular bin. No correction for detector effects is applied. The angular region of interest is between the most energetic jet, by definition at azimuthal angle $\phi = 0°$, and the second most energetic jet, mostly found around 160°-170°. The gluon jets are seen as a hump above 180°. (The position of the hump depends on the value of y_{cut} used.) It is seen that the density of particles between jets 1 and 2 is markedly smaller in the case of $\mathrm{q\bar{q}g}$ events (open points) than in the case of the $\mathrm{q\bar{q}}\gamma$ events (solid points): this difference in the particle densities of the two event types is the string effect, which is thus clearly observed in our data.

For the purposes of discussion of systematic effects and the comparison to model calculations it is useful to quantify the observed string effect. First, the "reduced angle" $X = \phi_{i-j1}/\phi_{j1-j2}$ is defined, as in ref. [12–14], as the ratio of the azimuthal angle of charged tracks i between jets 1 and 2, to the angle between the directions of the two highest energy jets, calculated event by event. The ratio R of charged particle density in three-jet to two-jet radiative events, in the range $0.3 < X < 0.7$, will serve as a measure of the string effect. From the reference case of fig. 1a, the histogram of fig. 1b is constructed, yielding a value

$$R = \frac{n_{\mathrm{q\bar{q}g}}(0.3 < X < 0.7)}{n_{\mathrm{q\bar{q}}\gamma}(0.3 < X < 0.7)} = 0.71 \pm 0.03$$

where the error is statistical. This ratio is expected to be insensitive to detector effects in first order since they are common to both numerator and denominator. The size of the effect is about the same magnitude as was observed at around 30 GeV centre of mass energy [12–14].

3.1 Systematic Effects

Several possible sources of systematic error were studied. In particular, the sensitivity of the results to the gluon jet identification technique was examined, as well as the effect of the kinematic differences between $q\bar{q}g$ and $q\bar{q}\gamma$ events and the jet clustering algorithm. The results are summarized in table 1.

3.1.1 Gluon Jet Identification

The energy ordering technique does not provide perfect discrimination between gluon and quark jets. As a consequence, the apparent depletion of particle flow between quark jets in $q\bar{q}g$ events is reduced by the misidentification of quark and gluon jets. In an attempt to estimate the importance of this misidentification, Monte Carlo events with full detector simulation were used. With the ERT $\mathcal{O}(\alpha_s^2)$ matrix element calculation [22], as implemented in JETSET [23], with parameters tuned to OPAL measurements of event shapes in [24], the gluon jet was defined as the one closest in direction to the primary gluon, once generated events with two or four primary partons ($\sim 20\%$ of the events) had been rejected. From this model, for events which pass the selection criteria, the purity of the gluon identification using the lowest energy jet was estimated to be 80.1 ± 0.2 % (statistical error). Fig. 2 shows the charged particle flow in three-jet events as predicted by the ERT model. The solid histogram shows this flow when the lowest energy jet is taken to be the gluon jet, as for the data, and the dashed histogram when the Monte Carlo generator information is used to tag the gluon jet, as described above. Based on this method of gluon jet identification, and to the extent that the matrix element Monte Carlo with string fragmentation gives a good representation of the data, the ratio of these two $q\bar{q}g$ particle flows, 0.72 ± 0.03, is seen as a correction factor for gluon jet identification to be applied to the ratio R defined above. This result suggests that the impurity in the gluon jet identification acts to dilute the string effect.

This conclusion is supported by a second method which uses data to enrich the purity of the gluon jet sample. Lepton-tagged $q\bar{q}g$ events were used as a reference sample where the gluon-jet identification was high. Energetic leptons originate mostly from semileptonic b decays. Therefore, as in ref. [2], if an electron or muon was identified in one of the two lower energy jets, the gluon jet was considered to be the untagged lower energy jet. The lepton tagging was based on a procedure described in ref. [25], with the additional requirement that the electron should have a minimum momentum of 2 GeV/c, and a muon a minimum of 3 GeV/c. By the method based on $\mathcal{O}(\alpha_s^2)$ matrix element Monte Carlo described above, the purity of the gluon tag was estimated to be $91.1 \pm 1.2\%$. The measured ratio of these two $q\bar{q}g$ particle flows in this case is 0.85 ± 0.01.

3.1.2 Kinematic Effects

- To first order in α or α_s, the angular distribution of a radiated photon from a massless quark is the same as that of a radiated gluon. However, because of higher order effects in QCD, the non-zero mass of the gluon jet, initial-state radiation, event selection criteria or other detector effects, the distribution of opening angles between the two quark jets may not be identical in the $q\bar{q}g$ and $q\bar{q}\gamma$ samples causing biases. Fig. 3 shows a detailed view of the angle of the second jet with respect to the first. For the case considered, $y_{cut}= 0.007$, it is seen that the difference in the mean quark jet opening angle is negligible: $0.35°$.

- As has been remarked in ref. [8], the difference in invariant mass between the gluon jet and the photon leads to a different energy scale for the two types of events considered, given the same topology. This may raise questions on the validity of the comparison. The argument, however, is expected to become weaker at LEP energies than around 30 GeV because of the larger jet energies. Note that in the perturbative approach, Dokshitzer *et. al.* [4,26] claim that, because of colour conservation, the interjet angular distribution is insensitive to the masses of the jets. The kinematic difference between the two samples of data is illustrated in fig. 4, which shows the mean of the summed energy of the first two jets as a function of their opening angle, for each of the two samples. With the same opening angle, the sum of the quark jet energies is on average about 4 GeV (or 6%) larger in the $q\bar{q}\gamma$ data than in the $q\bar{q}g$ data. Such a difference in energy increases the multiplicity of a jet by about 4% [27]. This was confirmed by Monte Carlo simulation study, without detector simulation, where the centre of mass energy of the $q\bar{q}g$ sample was artificially raised to correct for this kinematic difference. This is clearly insufficient to explain the $\sim$ 30% string effect observed.

With the representation in terms of the reduced angle, X, one can evaluate the possible sensitivity to kinematic effects by constructing histograms for restricted ranges of energy, 8-14 GeV and 14-28 GeV, for the photon and for the gluon jet. This is shown in fig 5. The two different ranges of energy for the third jet (either "gluon" or γ) yield $R = 0.60 \pm 0.03$ and 0.73 ± 0.04, respectively. Thus, the string effect is present in both energy ranges. It is larger for events with a soft third jet (or photon). Apart from possible kinematic conditions, the higher purity of gluon-jet identification for events with a soft third jet (92% and 74% in the two intervals, according to the model of estimation of sect. 3.1.1, and calculated correction factors 0.83 and 0.70 respectively) constitutes an explanation of this observation.

3.1.3 Quark Flavour Composition

It was verified using JETSET without detector simulation that no significant bias was introduced by the fact that the quark flavour composition is different in $q\bar{q}g$ and $q\bar{q}\gamma$

events: the ratio of particle flows of a $q\bar{q}g$ sample generated with decays $Z \to b\bar{b}$ only to that from a sample consisting of a mixture of $Z \to q\bar{q}$ decays was 0.986 ± 0.030.

3.1.4 Jet Clustering

Associated with the choice of the y_{cut} value are systematic effects related to the jet definition and the event kinematics.

With the Durham jet clustering algorithm, as with other invariant mass jet algorithms used in e^+e^- collision physics, all particles are assigned to a jet. Thus, depending on the choice of y_{cut}, interjet particle flow could be reconstructed as a third (or fourth) jet in a $q\bar{q}\gamma$ (or $q\bar{q}g$) event, causing it to be rejected. It is expected that this will be more likely in $q\bar{q}\gamma$ events because of the larger particle density between the jets. This would lead to a decrease in the observed string effect. This was tested by analysing a sample of events where fourth jets found by the Durham algorithm were accepted, but considered to be interjet particle flow, rather than as a separate jet, if they consisted of four or fewer particles. The measurement of the string effect is enhanced in this case from $R = 0.71 \pm 0.03$ to $R = 0.67 \pm 0.04$.

As the value of y_{cut} is varied, the kinematics of the events are changed: because of the isolation requirement of the photon, and the width of the intrajet flow, the distribution of opening angles (fig. 3) between the quark jets may differ between $q\bar{q}\gamma$ and $q\bar{q}g$ events, and particles belonging to the gluon jet may enter into the interquark region for values of y_{cut} lower than that used in this analysis. More significantly, the efficiency of the energy ordering method for the identification of gluon and quark jets varies with y_{cut} since the energy distribution of the partons changes: the gluon purities, as estimated by the model of sect. 3.1.1, decrease from 82% to 76% for y_{cut} values of 0.005 to 0.025 respectively.

The observed magnitude of the string effect was found to have a weak negative correlation with the value of y_{cut} used (see table 1). This weak dependence is dominated by the gluon jet identification purity.

As a cross check, and to separate clearly between intrajet (within a single jet) and interjet (between two jets) regions, a cone algorithm for jet clustering [28] was used. Here, a jet is defined as a group of particles clustered spatially within a cone, and not all particles are necessarily assigned to jets. Thus, the interjet particle flow does not enter into the jet 4-momentum definition. For this study, the half-angle of the cone was taken to be 0.7 radians, as recommended in ref. [28], while the minimum energy of the jet was taken to be 7.5 GeV, in order to be consistent with the cut on the photon energy. A value of $R = 0.74 \pm 0.04$ is obtained when the cone algorithm is used with these parameters, consistent with the reference value based on $y_{cut} = 0.007$ for the Durham algorithm.

3.1.5 Momentum Dependence

In previous studies at lower energies [1, 13, 14], it was found that the string effect was enhanced when a cut was applied on p_{out}, the charged particle momentum components out of the event plane. This was predicted by the Lund model [3]. It is a simple consequence of the Lorentz boost of the string fragments joining the gluon and the quarks, from their proper frame to the centre of mass of the whole $\mathrm{q\bar{q}g}$ system. In addition, massive resonance decays are expected to contribute to charged particle density in the out-of-plane region. For low p_{out}, and at low centre of mass energies, the decay daughters do not always follow the direction of the parent, and the string effect is diluted. The phenomenon must therefore be more pronounced for particles with larger mass, or larger momentum transverse to the boost direction.

For this study of momentum dependence, the selection of charged particles in the $\mathrm{q\bar{q}g}$ and $\mathrm{q\bar{q}}\gamma$ samples allowed transverse momenta $p_T > 0.15$ GeV/c, but the particle flow histograms were constructed only for particles having a given minimum value of momentum p or out-of-plane momentum p_{out}. As the momentum cuts of charged particles were raised from 0.15 GeV/c to 0.5 GeV/c, the ratio R of particle flows was found to vary between 0.76 ± 0.03 and 0.66 ± 0.03, but with correction factors for gluon identification estimated to be 0.75 ± 0.01 and 0.63 ± 0.02 respectively. Putting a cut on out-of-plane charged particle momentum appears to enhance the effect less significantly: $R = 0.71 \pm 0.04$ for $p_{out} > 0.3$ GeV/c (with correction factor 0.66 ± 0.02). These results are consistent with the prediction of ref. [6], which states that there should be little enhancement of the string effect for large particle momenta out of the plane, at LEP energies.

4 Comparison to Models

4.1 Monte Carlo Models

Using full detector simulation in all cases, the following models were studied:

- JETSET 7.3 [23] with the option of a coherent parton shower model and string fragmentation, with parameters tuned to OPAL data [29].
- HERWIG 5.5 [30], a parton shower model, with full treatment of coherence, with default parameters also obtained by tuning to OPAL event shapes. The hadronization proceeds from colourless clusters of quarks.
- ARIADNE 4.0 [31], based on a dipole model of gluon radiation and string fragmentation.

- COJETS 6.23 [32], which is based on an incoherent parton shower model with independent fragmentation, but uses different fragmentation parameters for gluon and quark jets.
- JETSET 7.3 [23] with the ERT matrix element option, and string fragmentation, with parameters tuned to OPAL event shapes [24]. With this model, only $q\bar{q}g$ events were generated.

The ratios of the two particle flows as a function of the reduced angle X for the various models are shown in fig. 6 and summarized in table 2.

The string effect is well reproduced by JETSET, with coherent parton shower evolution and string fragmentation. HERWIG shows a small, though significant deviation, possibly due to the model of cluster fragmentation used. Of the above Monte Carlo models, COJETS compares poorly with data, indicating that tuning of fragmentation parameters to event shapes is insufficient to reproduce the string effect in a model with an incoherent parton shower and independent fragmentation.

Having applied the same method of analysis to these samples of real and simulated data, the systematic errors will be the same, to first order, in the comparison of the various models. To quantify the measurements, the ratio R defined in sec. 3 is shown in fig. 7. Again, it is clearly demonstrated that only the incoherent parton shower model with independent fragmentation, COJETS, has a large disagreement with data. The same figure shows the dependence on y_{cut} for the data.

The relative importance of the perturbative and nonperturbative phases of the evolution of the hadronic events was investigated using Monte Carlo. For this purpose, $q\bar{q}g$ and $q\bar{q}\gamma$ events were generated using JETSET, but were not subjected to the detector simulation. Four cases were investigated: (i) coherent parton shower, with string fragmentation, as had been used above with full simulation, (ii) incoherent parton shower, with string fragmentation, using the tuned parameters of ref. [33], (iii) coherent parton shower, with independent fragmentation, using the tuned parameters of ref. [34], and (iv) incoherent parton shower, with independent fragmentation using the tuned parameters of ref. [34]. The charged particle flow was calculated in each case, using cuts similar to those applied to the data: only charged particles having $p_T > 0.25$ GeV/c were used (but jet reconstruction was based on all particles); the photon must have energy greater than 7.5 GeV, but less than either of the other two jets; a minimum of 4 particles was required per jet; and the angular region of the third jet was restricted to $|\cos(\theta_3)| < 0.82$. The resulting R ratios are shown in table 1. The first of these cases confirms that detector effects are small, since the R ratio, with full detector simulation, was 0.76 ± 0.03. On the basis of these models, it is concluded that the observed depletion in particle flow can be reproduced only if both interference effects in the parton shower development and nonperturbative effects represented by string fragmentation are used. In the cases with independent fragmentation, not only were the R ratios close to unity, but the absolute density of particle flow in the interquark region was approximately 70% too high, meaning that the parameter tuning by fitting general event shapes does not succeed in reproducing the interquark valley. It was verified that the difference in the tunes, for the first two cases, of the invariant mass cutoff of parton showers below which partons are not allowed to radiate gluons or photons did not significantly change the R ratio.

4.2 Coherence and LPHD

It is interesting to go one step further in the comparison of data to theory, after making simple assumptions. Azimov *et al.* [4] have calculated expressions valid to first order for the angular distribution of soft gluons emitted in the interjet region for the case of $\mathrm{q\bar{q}}\gamma$ and $\mathrm{q\bar{q}g}$ events. In the spirit of the LPHD hypothesis, the shape of the distribution of recorded hadrons can be identified as that of soft gluons.

The analytic expressions of ref. [4] represent interjet flow of soft gluons projected into the plane of a $\mathrm{q\bar{q}g}$ or $\mathrm{q\bar{q}}\gamma$ event, as a function of the angles between the hard partons (or photon). Gaussians centred around jet 1 and jet 2 were added to account for supplementary intrajet flow (within a jet):

$$\mathcal{F}(\phi) = P_1 \times \mathcal{A}(\mathrm{q\bar{q}g}\ or\ \mathrm{q\bar{q}}\gamma) + P_2 \times (N(0, P_3) + N(\theta_{j_1 j_2}, P_3)), \tag{1}$$

where $\mathcal{A}(\mathrm{q\bar{q}g}\ or\ \mathrm{q\bar{q}}\gamma)$ is the expression of Azimov *et. al.* [4] for the flow of soft gluons in $\mathrm{q\bar{q}g}$ or $\mathrm{q\bar{q}}\gamma$ events, and $N(\mu, \sigma)$ is a normal distribution centred at μ and with standard deviation σ. The distributions $\mathcal{A}$ are expressed as:

$$\begin{aligned} \mathcal{A}(q\bar{q}\gamma) &= 2C_F a_{+-} V(\phi, \beta) \\ \mathcal{A}(q\bar{q}g) &= N_c[a_{+1}V(\phi,\delta) + a_{1-}V(\beta,\delta)] + (2C_F - N_c)a_{+-}V(\phi,\beta). \end{aligned} \tag{2}$$

The colour factor C_F and the number of colours N_c are respectively 4/3 and 3 and

$$V(\phi, \beta) = \frac{2}{\cos\phi - \cos\beta}\left(\frac{\pi - \phi}{\sin\phi} - \frac{\pi - \beta}{\sin\beta}\right), \tag{3}$$

where ϕ is the angle between the quark(+) and the soft gluon, β the angle between the soft gluon and the anti-quark(−), δ the angle between the hard gluon (1) and the soft gluon, and where $a_{ik} = 1 - (\boldsymbol{n_i} \cdot \boldsymbol{n_k})$. The unit vector $(\boldsymbol{n_i})$ represents the direction of parton i.

A fit of the three parameters P_1, P_2 and P_3 of equation 1 was made for the particle flow between the quark jets in the range $10° < \phi < 150°$. The experimental curves were corrected for detector effects and for gluon purity using, as correction factors, the ratios of Monte Carlo particle flow distributions with and without detector simulation (JETSET parton shower model) and distributions with and without gluon tagging (JETSET with ERT model, without detector simulation, and with the requirement that the gluon jet be the least energetic jet). To perform this fit, the distribution of angles between jets (or the photon) in the data samples of selected q$\bar{\text{q}}$g and q$\bar{\text{q}}\gamma$ data was used when calculating the particle flow function $\mathcal{F}(\phi)$. The parameter $P_1 = 0.024 \pm 0.001$ (stat. error) is a coefficient to the expression for the angular distribution of soft gluon emission, $\mathcal{A}$, in the interjet region. Since this expression is normalized in the same way for q$\bar{\text{q}}$g and q$\bar{\text{q}}\gamma$ events, P_1 serves as a common scaling factor. The parameter $P_2 = 1.9 \pm 0.1$ represents a number of charged particles in the intrajet region, added to the general expression for the particle flow, and $P_3 = 0.22 \pm 0.01$ represents a characteristic mean angular width of a gaussian for this intrajet flow, in radians. Fig. 8 shows the form of the curves with the same values for the parameters, obtained by fitting both distributions simultaneously. Based on the quality of the reproduction of the shape and relative normalisation of the two curves, one could conclude, as in ref. [4], that with the LPHD the string effect is largely explained by simple coherence effects. This would be consistent with the predictions of ref. [6], but it cannot be ruled out that the observed effect could be due to other sources as well.

5 Conclusion

The string effect has been studied by a method which allows direct comparison of the particle flow in the interquark regions for two sets of data: three-jet multihadronic events, and events comprising two jets and an isolated photon. It is demonstrated that, in the former, there is a depletion between the two most energetic jets, assumed to be the quark jets, relative to the latter. With the jet definition based on the Durham algorithm, and a value of y_{cut}= 0.007, the ratio R of charged particle flows in three-jet and two-jet radiative events in a range of reduced angle $0.3 < X < 0.7$ was found to be 0.71 ± 0.03. The magnitude of the ratio of particle flows is about the same as was observed previously at lower energies, but the dependence on out-of-plane momentum is smaller, as predicted by ref. [6]. Studies of systematic effects are summarized in table 1.

The importance of the purity of the gluon jet identification was studied using lepton-tagging and Monte Carlo methods for identifying the quark jets. As expected, the depletion of the particle flow in q$\bar{\text{q}}$g events relative to q$\bar{\text{q}}\gamma$ events was found to be enhanced for samples with higher gluon purity.

The kinematic differences between the two types of events, as discussed in ref. [8], arising in particular from the mass of the gluon jet, have been shown to be insufficient to explain the observed effect. Acceptance effects, as well as dependencies on the reconstructed energy of the third jet are small. Systematic checks on the effects of different schemes of jet clustering, and on different values of the jet-clustering parameter have been performed.

The string effect is reproduced by coherent parton shower Monte Carlo calculations with string fragmentation (or cluster fragmentation, as implemented in HERWIG), but is poorly represented by incoherent parton shower models, even with tuned parameters. At generator level, the JETSET Monte Carlo suggests that angular ordering and azimuthal asymmetries in gluon radiation contribute partly to the string effect, and that independent fragmentation, with parameters tuned for general event shapes, does not reproduce the particle flow in the interquark region.

The qualitative features of the string effect are found to be reasonably reproduced by a model based on QCD calculations of soft gluon emission, under the assumption of the LPHD hypothesis.

Acknowledgements

It is a pleasure to thank the SL Division for the efficient operation of the LEP accelerator, the precise information on the absolute energy, and their continuing close cooperation with our experimental group. In addition to the support staff at our own institutions we are pleased to acknowledge the
Department of Energy, USA,
National Science Foundation, USA,
Particle Physics and Astronomy Research Council, UK,
Natural Sciences and Engineering Research Council, Canada,
Fussefeld Foundation,
Israel Ministry of Science,
Israel Science Foundation, administered by the Israel Academy of Science and Humanities,
Minerva Gesellschaft,
Japanese Ministry of Education, Science and Culture (the Monbusho) and a grant under the Monbusho International Science Research Program,
German Israeli Bi-national Science Foundation (GIF),
Direction des Sciences de la Matière du Commissariat à l'Energie Atomique, France,
Bundesministerium für Forschung und Technologie, Germany,
National Research Council of Canada,
A.P. Sloan Foundation and Junta Nacional de Investigação Científica e Tecnológica, Portugal.

Reference value	
y_{cut}= 0.007	0.71±0.03
purity of gluon id	
lepton-antitagging	0.60±0.03
ERT with gluon id	0.51±0.03
ERT without gluon id	0.71±0.03
energy of third jet	
8 - 14 GeV	0.60±0.03
14 - 28 GeV	0.73±0.04
jet clustering	
y_{cut}= 0.005	0.71±0.03
y_{cut}= 0.010	0.73±0.03
y_{cut}= 0.015	0.76±0.03
cone	0.74±0.04
including fourth jet	0.67±0.03
momentum dependence	
$p > 0.15$ GeV/c	0.76±0.03
$p > 0.5$ GeV/c	0.66±0.03
$p_{out} > 0.3$ GeV/c	0.71±0.04

Table 1: Systematic effects on the ratio R of particle flows

Reference value	
Data	0.71±0.03
Monte Carlo, with detector simulation	
JETSET	0.76±0.03
ERT (Data $q\bar{q}\gamma$)	0.71±0.03
HERWIG	0.82±0.02
ARIADNE	0.70±0.03
COJETS	1.08±0.03
JETSET, without detector simulation	
coherent, SF	0.73±0.03
incoherent, SF	0.91±0.03
coherent, IF	1.01±0.03
incoherent, IF	1.11±0.03

Table 2: Ratio R of particle flows, compared to models

References

[1] A. Petersen, in *Elementary Constituents and Hadronic Structure*, ed. Tran Than Van (Editions Frontières, Dreux, 1980), p.505;
W. Bartel *et. al.*, JADE Collaboration, *Phys. Lett.* **B101** (1981) 129; *Z. Phys.* **C 21** (1983) 37; *Phys. Lett.* **B134** (1984) 275; *Phys. Lett.* **B157** (1985) 340
H. Aihara *et. al.*, TPC/2γ Collaboration, *Phys. Rev. Lett.* **54** (1985) 270; *Z. Phys.* **C 28** (1985) 31;
M. Althoff *et. al.*, TASSO Collaboration, *Z. Phys.* **C 29** (1985) 29

[2] M.Z. Akrawy *et al.*, OPAL Collaboration, *Phys. Lett.* **B261** (1991) 334

[3] B. Andersson, G. Gustafson, G. Ingelman, and T. Sjöstrand, *Phys. Rep.* **97** (1983) 33

[4] Ya.I. Azimov, Yu.L. Dokshitzer, V.A. Khoze and S.I. Troyan, *Phys. Lett.* **165B** (1985) 147

[5] Ya.I. Azimov, Yu.L. Dokshitzer, V.A. Khoze and S.I. Troyan, *Z. Phys.* **C27** (1985) 65

[6] V. Khoze and L. Lönnblad, Phys. Lett. **B241** (1990) 123

[7] P. Hoyer *et al.*, *Nucl. Phys.* **B161** (1979) 349;
A. Ali, E. Pietarinen, G. Kramer and J. Willrodt, *Phys. Lett.* **93B** (1980) 155

[8] G. Ballochi and R. Odorico (1989), *Nucl. Phys.* **B** 345 (1990) 173;
R. Odorico, *proc. of the XXVth Rencontre de Moriond*, Les Arcs, 1990, p.177

[9] R. Field and R.P. Feynman, *Nucl. Phys.* **B136** (1978) 1

[10] P.D. Acton *et al.*, OPAL Collaboration, *Z. Phys.* **C** 54 (1992) 193;
P. Mättig, *Proceedings of the Eighth Lake Louise Winter Institute*, Lake Louise, Feb. 1993

[11] Ya. I. Azimov *et al.*, *Yad. Fiz.* **43** (1986) 149; translated in *Sov. J. Phys.* **43** (1986) 95.

[12] H. Aihara *et al.* TPC/2γ Collaboration, *Phys. Rev. Lett.* **57** (1986) 945

[13] P.D. Sheldon *et al.*, MARK II Collaboration, *Phys. Rev. Lett.* **57** (1986) 1398

[14] F. Ould Saada *et al.*, JADE Collaboration, *Z. Phys.* **C39** (1988) 1

[15] M. Acciarri *et al.*, L3 Collaboration, *Phys. Lett.* **B345** (1995) 74

[16] K. Ahmet *et al.*, OPAL Collaboration, *Nucl. Inst. and Meth. in Phys. Res.* **A305** (1991) 275;
M. Arignon *et al.*, *Nucl. Inst. and Meth. in Phys. Res.* **A313** (1992) 103

[17] P. P. Allport *et al.*, *Nucl. Inst. and Meth. in Phys. Res.* **A324** (1993) 34
P. P. Allport *et al.*, *Nucl. Inst. and Meth. in Phys. Res.* **A346** (1994) 476

[18] G. Alexander *et al.*, OPAL Collaboration, *Z. Phys.* **C52** (1991) 175

[19] P. Acton *et al.*, OPAL Collaboration, Z. Phys. **C58** (1993) 405

[20] S. Catani et. al., *Phys. Lett.* **B269** (1991) 432;
S. Bethke, et. al., *Nucl. Phys.* **B370** (1992) 310

[21] J.D. Bjorken and S. Brodsky, *Phys. Rev.* **D1** (1970) 1416

[22] R.K. Ellis, D.A. Ross and A.E. Terrano, *Nucl. Phys.* **B178** (1981) 421

[23] T. Sjöstrand, *Comp. Phys. Comm.* **47** (1987) 347;
T. Sjöstrand and M. Bengtsson, *Comp. Phys. Comm.* **43** (1987) 367

[24] P.D. Acton et. al., OPAL Collaboration, *Phys. Lett.* **B276** (1992) 547

[25] P. D. Acton et. al., OPAL Collaboration, *Z. Phys.* **C58** (1993) 523

[26] Yu. L. Dokshitzer *et. al.*, *Basics of Perturbative QCD*, Editions Frontières, 1991

[27] P. Abreu *et al.*, DELPHI Collaboration, *Z. Phys.* **C50** (1991) 185

[28] J.E. Huth *et al.*, *Research Directions for the Decade*, Snowmass (1990) 134 (Ed. E.L. Berger; World Scientific, Singapore);
R. Akers *et. al* OPAL Collaboration, *Z. Phys.* **C63** (1994) 197

[29] M.Z. Akrawy *et al.*, OPAL Collaboration, *Z. Phys.* **C47** (1990) 505

[30] G. Marchesini and B.R. Webber, *Nucl. Phys.* **B310** (1988) 464;
G. Marchesini, B.R. Webber et al., *Comp. Phys. Comm.* **67** (1992) 465

[31] L. Lönnblad, *Comp. Phys. Comm.* **71** (1992) 15

[32] R. Odorico, *Comput. Phys. Commun.* **59** (1990) 527

[33] P.D. Acton et. al., OPAL Collaboration, *Z. Phys.* **C58** (1993) 207

[34] R. Akers et. al., OPAL Collaboration, *Z. Phys.* **C63** (1994) 363

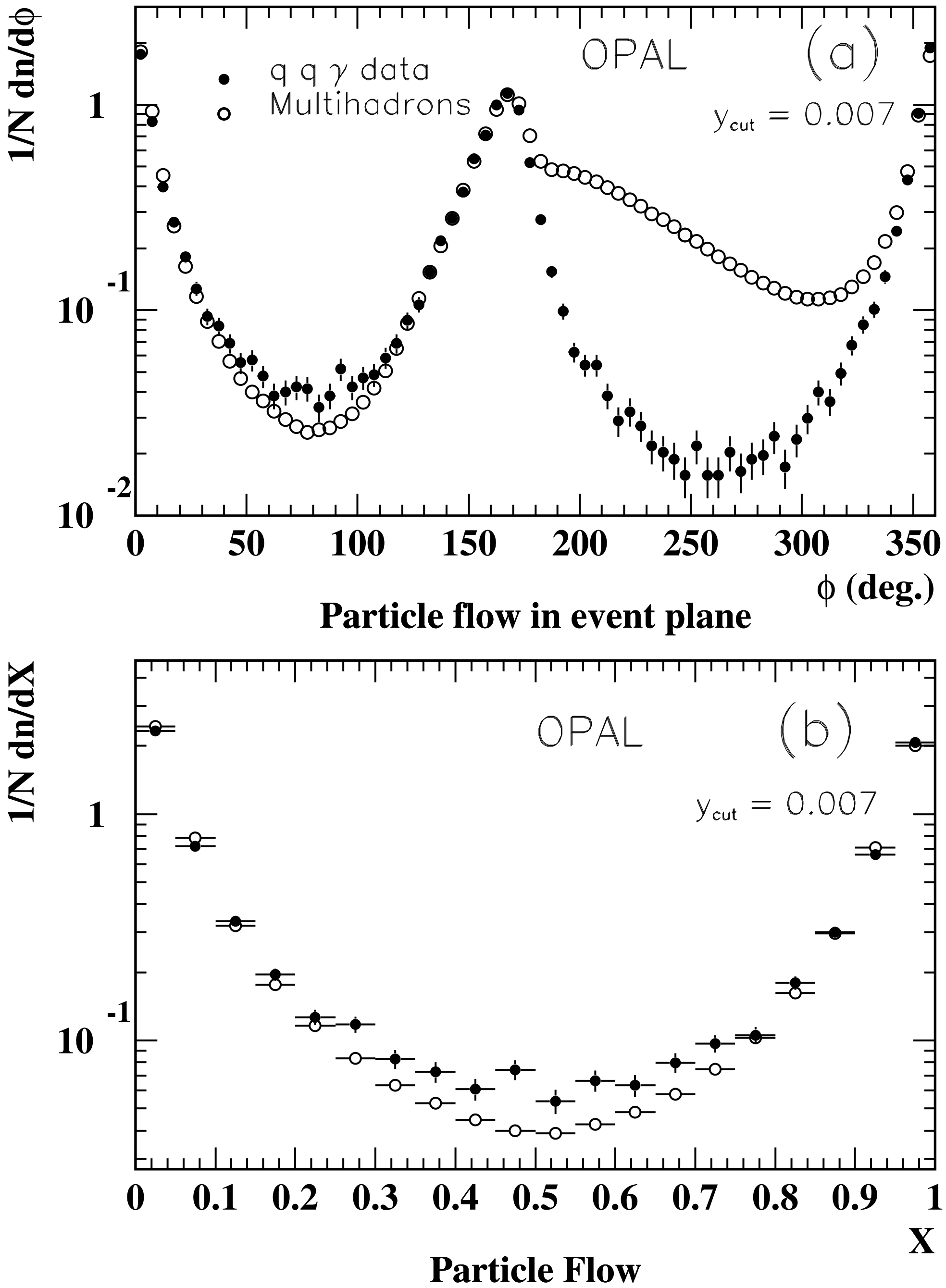

Figure 1: (a) Charged particle flow in the event plane for two-jet radiative events, and three-jet multihadronic events. Error bars for the $q\bar{q}g$ sample are smaller than the dots. (b) Charged particle flow with respect to the reduced angle X.

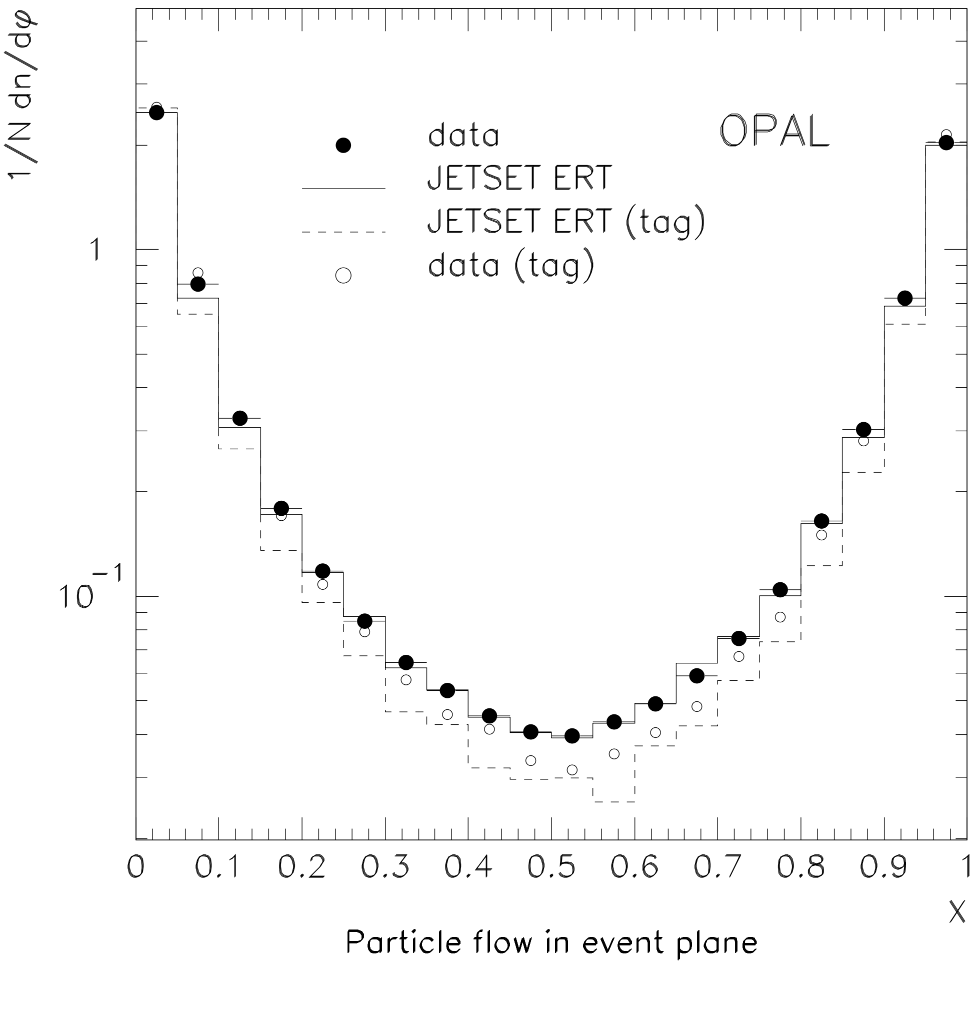

Figure 2: Particle flow in three-jet events with respect to the reduced angle X. Also shown are the predictions of the ERT matrix element Monte Carlo, taking the lowest energy jet to be the gluon jet, as for the data (solid histogram), and using the Monte Carlo generator information to tag the gluon jet, as described in the text (dashed histogram). The measurements from lepton-tagged data events, used to increase the gluon jet purity, are also shown.

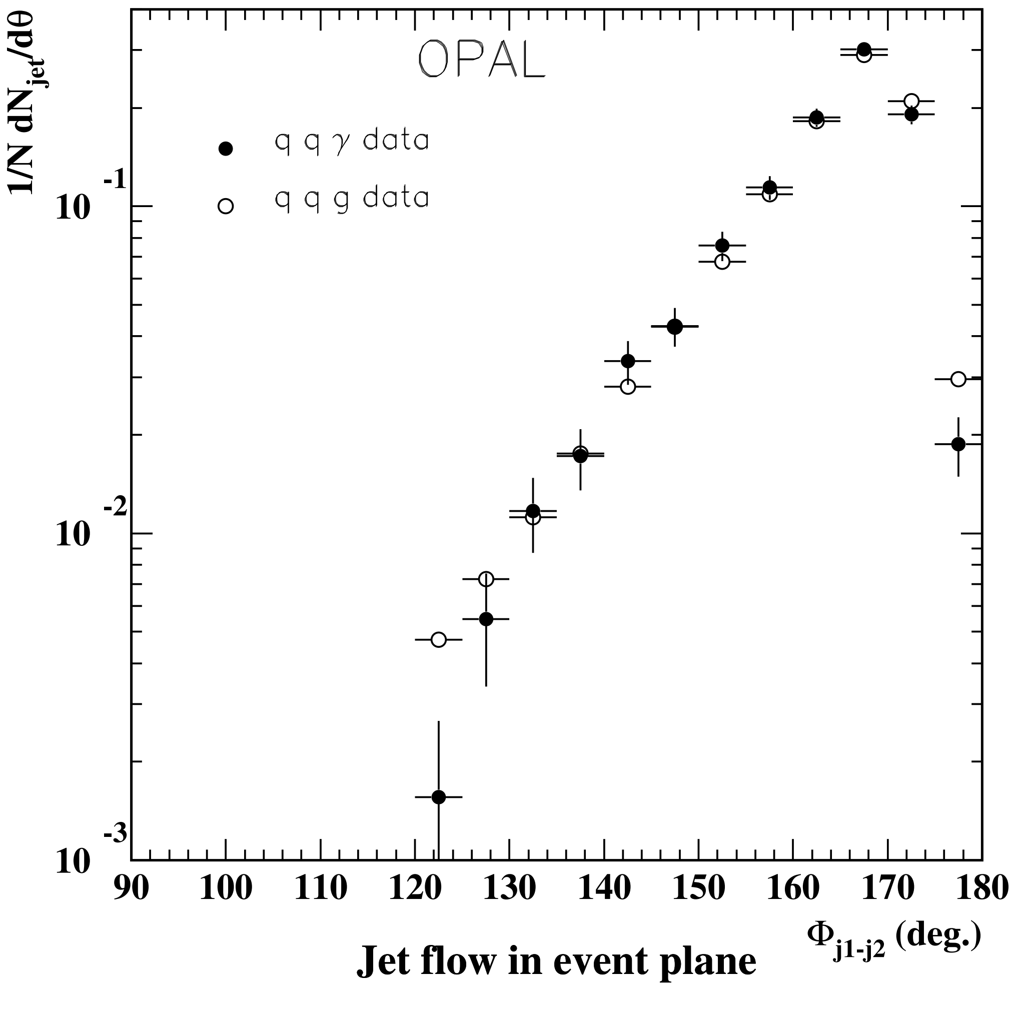

Figure 3: Angular distribution of the second jet with respect to the first for $q\bar{q}\gamma$ data as well as $q\bar{q}g$ data, with $y_{cut} = 0.007$. Note that the events were rejected if the angle between the two highest energy jets was below 120°.

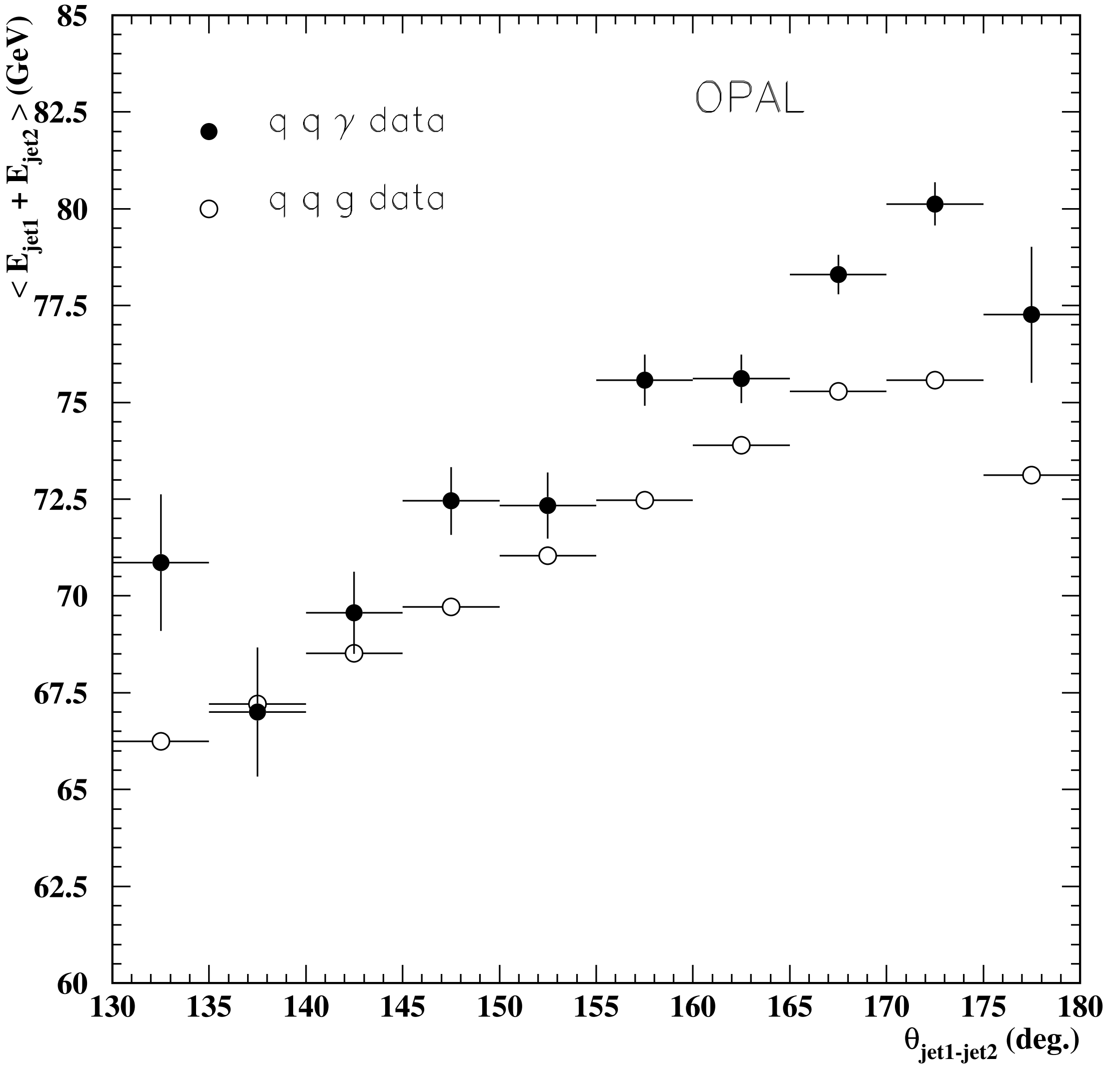

Figure 4: Mean value of the summed energy of the two "quark" jets as a function of their opening angle for three-jet hadronic events (open circles) and two-jet radiative events (filled circles). The vertical error bar shows the uncertainty in the mean value. The width of the summed energy distribution is 5-10 GeV, depending on the value of θ.

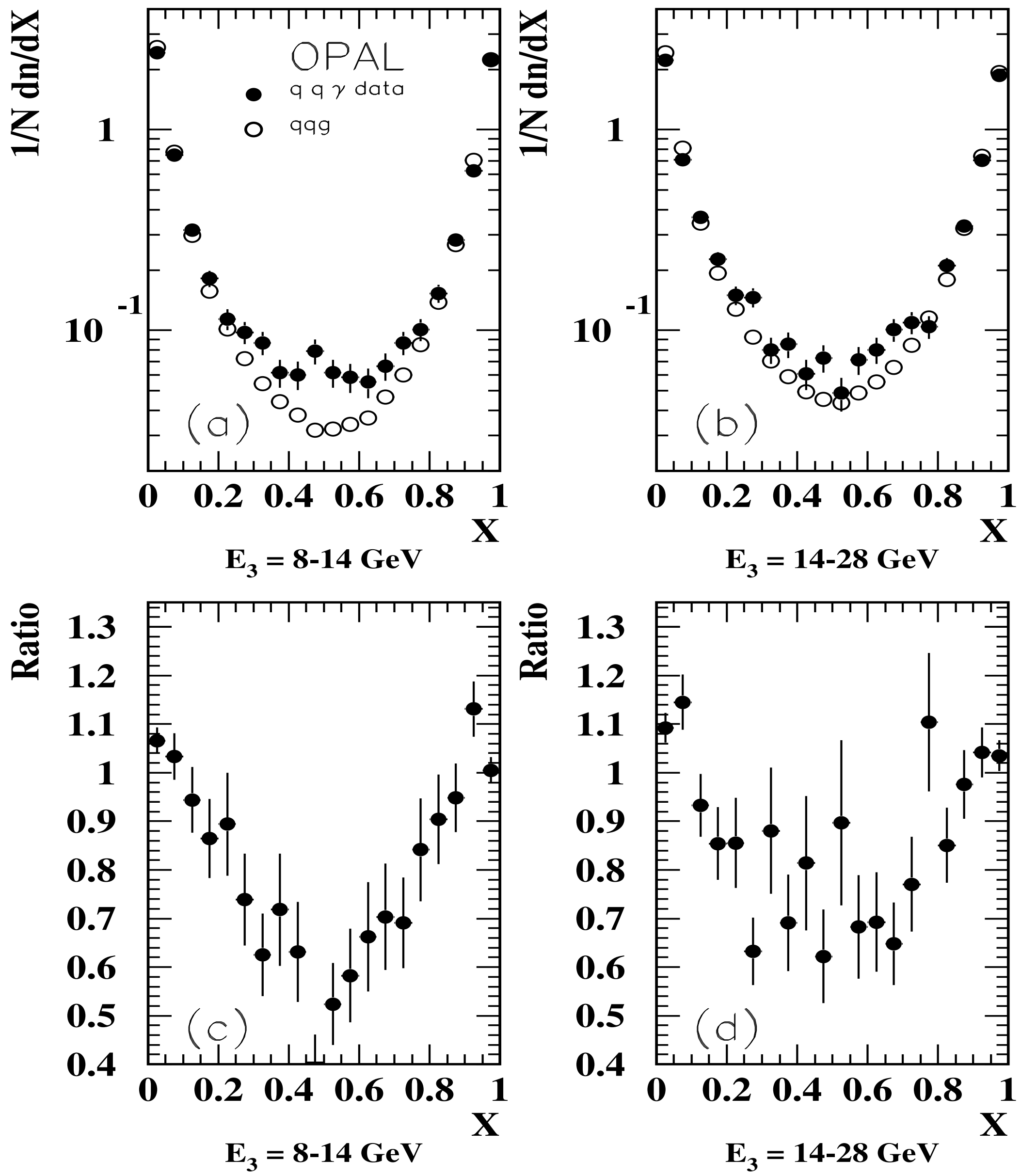

Figure 5: Charged particle flow in two ranges of γ(g) energies, with respect to the reduced angle X defined in the text. The bottom figures show the ratio of the two particle flows, illustrating the extent of the depletion in the $q\bar{q}g$ sample of data.

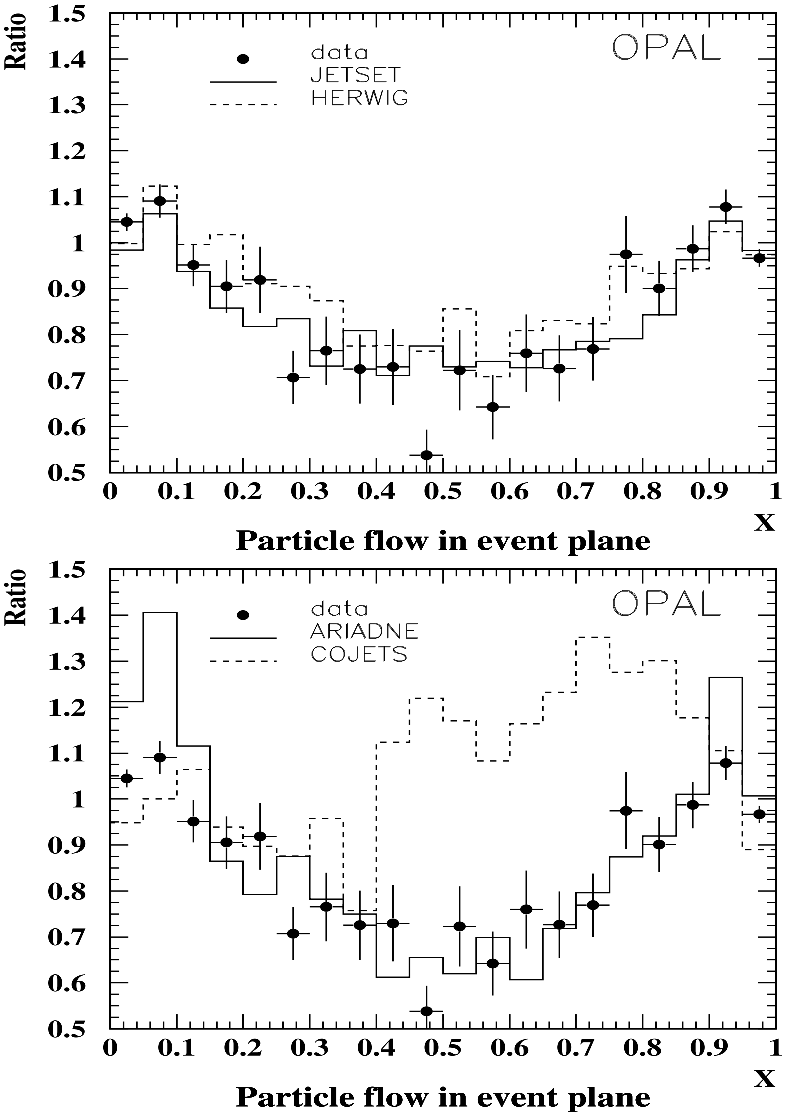

Figure 6: Ratio of charged particle flows in three-jet and two-jet radiative events with respect to the reduced angle X for various Monte Carlo models: JETSET coherent parton shower with string fragmentation, HERWIG, ARIADNE and COJETS.

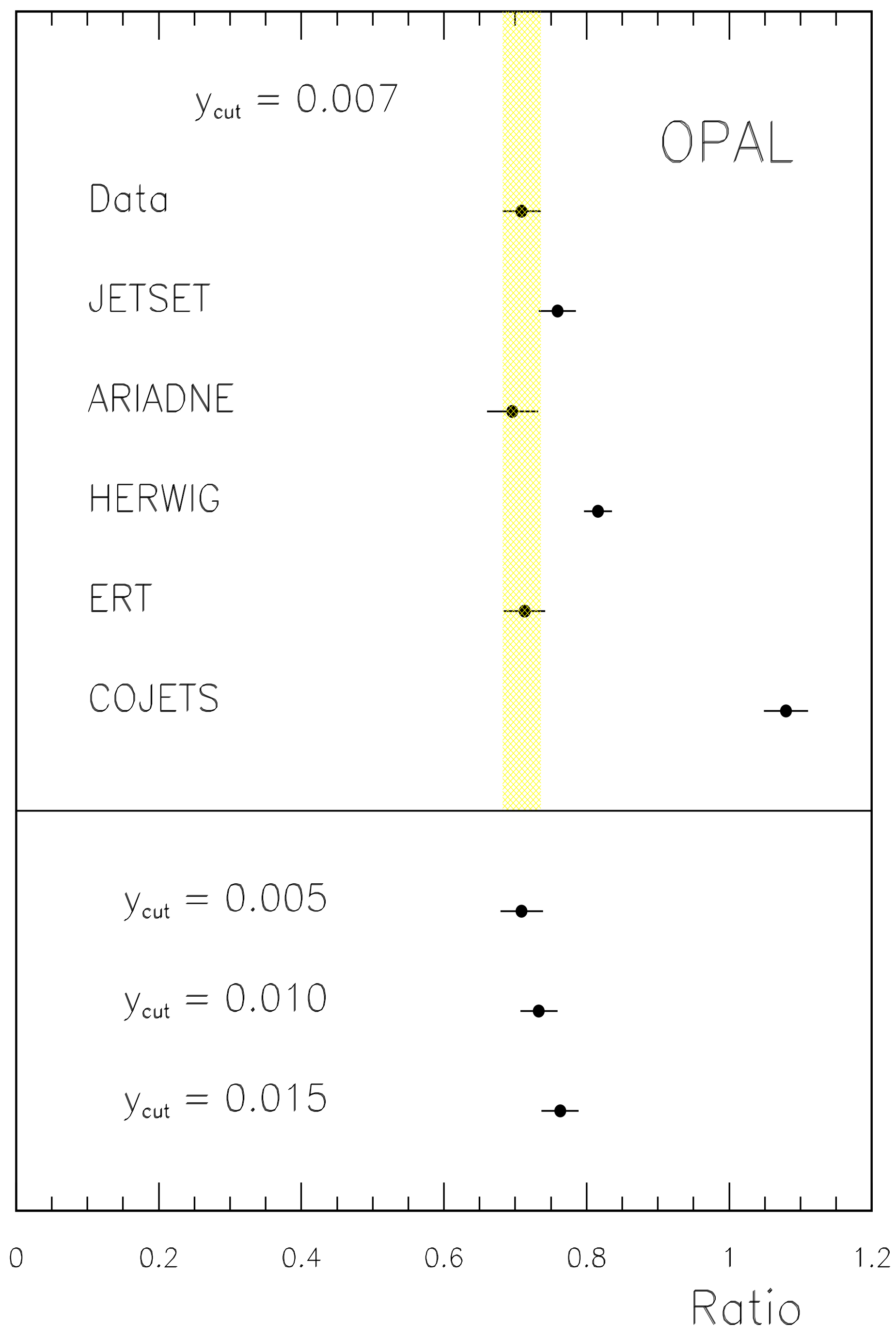

Figure 7: Mean value of the ratio of charged particle flows in three-jet and two-jet radiative events in the range $0.3 < X < 0.7$, for data (band) and various Monte Carlo models, with selection based on a fixed value of y_{cut}= 0.007. The error bars are statistical. For the ERT model, the $q\bar{q}\gamma$ sample used is selected from the data. Below the line are shown ratios for data, for different y_{cut} values.

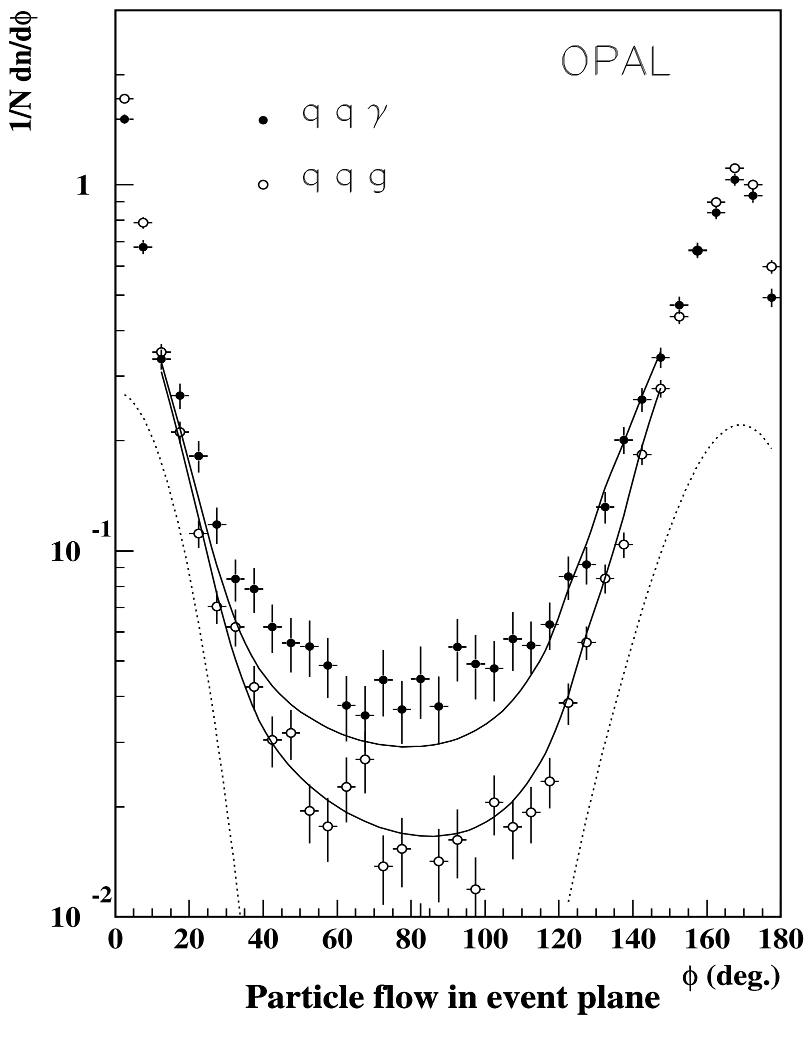

Figure 8: Fits of the charged particle flows to the expression (1) in the text. The dotted lines represent the additional contribution from the intrajet flow.